

High SNR Capacity of Millimeter Wave MIMO Systems with One-Bit Quantization

Jianhua Mo and Robert W. Heath, Jr.

Wireless Networking and Communications Group

The University of Texas at Austin, Austin, TX 78712, USA

Email: {jhmo, rheath}@utexas.edu

Abstract—Millimeter wave (mmWave) is a viable technology for future cellular systems. With bandwidths on the order of a gigahertz, high-resolution analog-to-digital converters (ADCs) become a power consumption bottleneck. One solution is to employ very low resolution one-bit ADCs. This paper analyzes the flat fading multiple-input multiple-output (MIMO) channel with one-bit ADC. Bounds on the high signal-to-noise ratio (SNR) capacity are derived for the single-input multiple-output (SIMO) channel and the general MIMO channel. The results show how the number of paths, number of transmit antennas, and number of receive antennas impact the capacity at high SNR.

I. INTRODUCTION

Millimeter wave (mmWave) is a technology that can provide high bandwidth communication links in cellular systems. As mmWave uses larger bandwidths, the corresponding sampling rate of the analog-to-digital converter (ADC) scales up. Unfortunately, high speed, high precision (e.g., 8-12 bits) ADCs are costly and power-hungry for portable devices [1], [2]. A possible solution is to use special ADC structures like a time-interleaved ADC (TI-ADC) architecture where a number of low-speed, high-precision ADCs operate in parallel. The main challenge of the TI-ADC is the mismatch among the sub-ADCs in gain, timing and voltage offset which can cause error floors in receiver performance [3], [4]. An alternative solution is to live with ultra low precision ADCs (1-3 bits), which reduces power consumption and cost.

In this paper, we investigate the capacity of multiple-input multiple-output (MIMO) system in which a one-bit ADC is used for each inphase and quadrature baseband received signal. The main advantage of this architecture is the ADCs can be implemented with very low power consumption [5]. The architecture also simplifies the overall complexity of the circuit for example automatic gain control may not be required [6]. Several aspects of one-bit ADCs have been investigated in prior work including the loss of the channel capacity [7]–[10], channel estimation [11], [12], synchronization [13], and MIMO channels with one-bit ADCs [14]–[17].

We study the channel capacity of the MIMO system with one-bit ADCs in the high SNR regime. When beamforming is at the transmitter, it is possible that mmWave systems will operate in medium or higher SNR regimes. Combining with results derived from the low SNR regime [15], [17], our results provide a more complete understanding of the impact of one bit quantization on the MIMO channel for the whole SNR regime. Note that ADCs transform continuous inputs into

discrete outputs. In the low SNR regime, this nonlinearity is tackled using linear approximation around zero [15]. In the high regime, the nonlinearity always exists in our analysis. This requires a different mathematical approach for the high SNR case.

We first study the high SNR capacity of SIMO channel with one-bit ADC and provide a closed form expression when the receiver has a large number of antennas. For the MIMO channel, we provide a bound for the high SNR capacity. Then these results for the general MIMO channels are applied to sparse mmWave channels. We propose a receiver structure where analog phase shifters are placed before one-bit ADCs. The phase shifters incur additional power consumption but improve performance in medium and high SNR regimes.

The work [15] is most related to the contribution of our paper. In [15], the mutual information of MIMO channel with one-bit ADCs in the low SNR regime up to second order of SNR is derived. It was found that under the constraint that each antenna transmits signals independently and with equal power, QPSK is the best signaling strategy. In addition, there is a reduction of low SNR channel capacity by factor $2/\pi$ (−1.96dB) due to one bit quantization. These results do not extend to the high SNR regime.

Notation : a is a scalar, \mathbf{a} is a vector and \mathbf{A} is a matrix. $\angle x$ represents the phase of a complex number x . $\Re(x)$ and $\Im(x)$ denote the real and imaginary part of x , respectively. $\mathbf{x}_{i:j}$ is the vector consisting of $\{x_k, i \leq k \leq j\}$. $\text{tr}(\mathbf{A})$, \mathbf{A}^T and \mathbf{A}^* represent the trace, transpose and conjugate transpose of a matrix \mathbf{A} , respectively. $\mathbf{A} \odot \mathbf{B}$ denotes the Hadamard product of \mathbf{A} and \mathbf{B} .

II. SYSTEM MODEL

Consider a MIMO system with one-bit quantization, as shown in Fig. 1. There are N_t antennas at the transmitter and N_r antennas at the receiver. Assuming perfect synchronization and a narrowband channel, the baseband received signal is,

$$\mathbf{y} = \mathbf{H}\mathbf{x} + \mathbf{n}, \quad (1)$$

where $\mathbf{H} \in \mathbb{C}^{N_r \times N_t}$ is the channel matrix, $\mathbf{x} \in \mathbb{C}^{N_t \times 1}$ is the signal sent by the transmitter, $\mathbf{y} \in \mathbb{C}^{N_r \times 1}$ is the received signal before quantization, and $\mathbf{n} \sim \mathcal{CN}(0, \mathbf{I})$ is the Gaussian noise. In our system, there are a total of $2N_r$ one-bit resolution quantizers that separately quantize the real and imaginary part of each received signal.

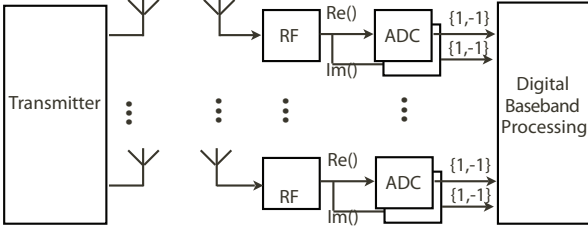


Fig. 1. System model.

We define a one-bit quantization function \mathbf{Q} as follows. Assume that $\mathbf{r} = \{r_i, 1 \leq i \leq N_r\}$ and $\mathbf{y} = \{y_i, 1 \leq i \leq N_r\}$. If

$$\Re(r_i) = \text{sgn}(\Re(y_i)), \quad (2)$$

$$\Im(r_i) = \text{sgn}(\Im(y_i)), \quad (3)$$

for $1 \leq i \leq N_r$, then we denote that $\mathbf{r} = \mathbf{Q}(\mathbf{y})$. Here, $\text{sgn}(x)$ is the sign function and $r_i \in \{1+j, 1-j, -1+j, -1-j\}$.

After the one-bit quantization at the receiver, we obtain the output $\mathbf{r} = \mathbf{Q}(\mathbf{y})$. Consequently, the channel capacity with one-bit quantization is

$$C = \max_{\mathbf{p}(\mathbf{x}) : \text{tr}(\mathbb{E}\{\mathbf{x}\mathbf{x}^*\}) \leq P} I(\mathbf{x}; \mathbf{r}) \quad (4)$$

where P is the average power constraint at the transmitter.

III. HIGH SNR CAPACITY OF MIMO CHANNEL WITH ONE-BIT QUANTIZATION

The mutual information in (4) is in the form of multiple integrals; obtaining a closed form expression for the optimization problem seems to be a challenge. Thus, we derive an approximation of the channel capacity in the high SNR regime.

A. SISO Channel with One-Bit Quantization

First, we deal with the very special case when $N_r = N_t = 1$. The channel coefficient now is a scalar denoted by h .

Lemma 1. *The capacity of the SISO channel with one-bit quantization is achieved by rotated QPSK signaling, i.e.,*

$$\Pr\{x = \sqrt{P}e^{j(k\pi + \frac{\pi}{4} - \angle h)}\} = \frac{1}{4}, \text{ for } k = 0, 1, 2, 3, \quad (5)$$

and is given by

$$C_{\text{SISO}}(P) = 2 \left(1 - H \left(Q(|h| \sqrt{P}) \right) \right), \quad (6)$$

where $H(p) = -p \log_2 p - (1-p) \log_2 (1-p)$ and $Q(\cdot)$ is the tail probability of the standard normal distribution.

Proof: Without loss of optimality, we can assume that the transmitted signal is $x = e^{-j\angle h} \hat{x}$. The outputs of the one-bit quantizer will be $\Re(r) = \text{sgn}(|h|\Re(\hat{x}) + \Re(n))$ and $\Im(r) = \text{sgn}(|h|\Im(\hat{x}) + \Im(n))$. Therefore, the channel is decoupled into two real channels with the same channel gain. For each real channel, it is proven in [8, Theorem 2] that binary antipodal signaling is optimal. Therefore, the optimal input for the SISO channel is rotated QPSK signaling. ■

As $P \rightarrow \infty$, it follows that $Q(|h|\sqrt{P}) \rightarrow 0$ and $\lim_{P \rightarrow \infty} C_{\text{SISO}}(P) = 2 \text{ bps/Hz}$.

B. SIMO Channel with One-Bit Quantization

In the SIMO channel with N_r antennas at the receiver, there are at most 2^{2N_r} possible quantization outputs. Therefore, 2^{2N_r} is a simple upper bound for the channel capacity. This upper bound, unfortunately, cannot be approached when N_r is larger than one, as shown in the following proposition.

Proposition 1. *The capacity of the SIMO channel with one-bit quantization at high SNR, denoted as $\bar{C}_{\text{SIMO}}(N_r)$, satisfies*

$$\log_2(4N_r) \leq \bar{C}_{\text{SIMO}}(N_r) \leq \log_2(4N_r + 1). \quad (7)$$

Proof: Denote the SIMO channel as $\mathbf{h} = [h_1, h_2, \dots, h_{N_r}]^T$. When the phase of the transmitted symbol x is around $\angle x = k\pi/2 - \angle h_i (k = 0, 1, 2, 3; i = 1, 2, \dots, N_r)$, one element of the one-bit quantization output will change its sign. There are at most $4N_r$ such phases, denoted as $\Phi = \{\phi_i, 1 \leq i \leq 4N_r\}$. Following the derivations in [7] and [9], it can be shown the high SNR capacity is achieved with transmit symbols from three categories:

- 1) The symbol zero;
- 2) The symbols with phases in Φ ;
- 3) The symbols with phases not in Φ .

For the zero symbol, $\Pr(\mathbf{r}|x = 0) = 2^{-2N_r}$ for each possible \mathbf{r} . For the symbols with phases not in Φ , $\Pr(\mathbf{r}|x) = 1(\mathbf{r} = \mathbf{Q}(\mathbf{h}x))$ where $1(\cdot)$ is the indicator function. At last consider the symbols with phases in Φ . If $\angle x = -\angle h_1$, then $\Pr(\mathbf{r} = [1+j, \mathbf{Q}(\mathbf{h}x)_{2:N_r}^T]^T | x) = \Pr(\mathbf{r} = [1-j, \mathbf{Q}(\mathbf{h}x)_{2:N_r}^T]^T | x) = 1/2$. The other conditional probabilities can be derived similarly. Therefore, the transition probability matrix from these three kinds of input symbols to the output is

$$\Pr(\mathbf{r}|x) = \begin{bmatrix} 2^{-2N_r} \dots & \dots 2^{-2N_r} \\ \mathbf{T}_{4N_r \times 4N_r} & \mathbf{0}_{4N_r \times (2^{2N_r} - 4N_r)} \\ \mathbf{I}_{4N_r \times 4N_r} & \mathbf{0}_{4N_r \times (2^{2N_r} - 4N_r)} \end{bmatrix} \quad (8)$$

where \mathbf{T} is a $4N_r \times 4N_r$ circulant matrix with the first row as $[1/2, 1/2, 0, \dots, 0]$.

Assume that these three kinds of symbols are transmitted with probabilities p_0, p_1 and $1 - p_0 - p_1$, respectively. The resulting mutual information, denoted as $f(p_0, p_1)$, is as shown at the top of the next page. The channel capacity can be computed by searching the optimal p_0 and p_1 , denoted as p_0^* and p_1^* , which maximizes the mutual information $f(p_0, p_1)$. It turns out that $\partial f(p_0, p_1) / \partial p_1 < 0$ and thus $p_1^* = 0$. Therefore, there are at most $4N_r + 1$ possible input symbols in the capacity-achieving distribution and an upper bound of the capacity is $\log_2(4N_r + 1)$. The lower bound $\log_2(4N_r)$ is achieved by setting $p_0 = 0$ and $p_1 = 0$, i.e., $f(0, 0) = \log_2(4N_r)$. ■

Corollary 1. *When N_r is large, the capacity of SIMO channel with one-bit quantization at high SNR is*

$$\bar{C}_{\text{SIMO}}(N_r) \approx \log_2(4N_r + 1). \quad (10)$$

Proof: When N_r is large,

$$f(p_0, 0) \approx -(1 - p_0) \log_2 \frac{1 - p_0}{4N_r} - p_0 \log_2 p_0.$$

$$f(p_0, p_1) := \left(-1 + p_0 - p_1 - p_0 \frac{4N_r}{4N_r}\right) \log_2 \left(\frac{1 - p_0 - p_1}{4N_r} + \frac{p_0}{4N_r} + p_1\right) - 2p_1 - \frac{8N_r^2}{4N_r} p_0 - \frac{4N_r - 4N_r}{4N_r} p_0 \log_2 p_0 \quad (9)$$

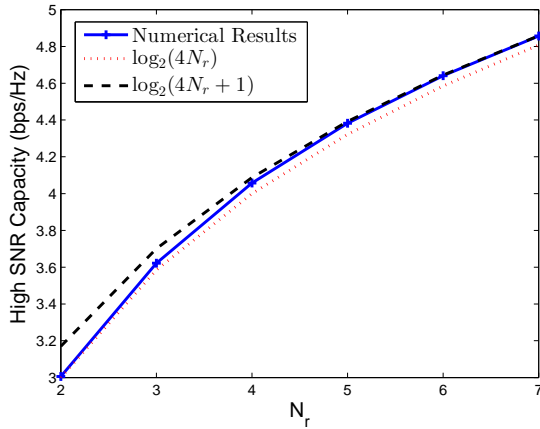


Fig. 2. The high SNR capacity and its lower bound and upper bound.

It turns out that $p_0^* = \frac{1}{4N_r+1}$ and $f(p_0^*, 0) \approx \log_2(4N_r + 1)$. ■

In Fig. 2, we plot the high SNR capacity obtained by numerically maximizing the mutual information function $f(p_0, p_1)$. The lower bound $\log_2(4N_r)$ and upper bound $\log_2(4N_r + 1)$ are also plotted. It is shown that the high SNR capacity converges to $\log_2(4N_r + 1)$ when $N_r \geq 6$.

For the special case when $\angle h_m = \angle h_n + k\pi/2$, $k \in \{0, 1, 2, 3\}$ for some $m \neq n$, the total number of distinguishable input symbols will be less than $4N_r$. We usually assume that the channel coefficients are generated from continuous distribution. Thus with probability one, $\angle h_m \neq \angle h_n + k\pi/2$, $k \in \{0, 1, 2, 3\}$ for $m \neq n$.

In many systems, the zero symbol is not included as part of the constellation due to peak-to-average power ratio (PAPR) issues. Therefore, in the high SNR regime, only $4N_r$ distinguishable symbols are employed as the channel inputs and there will be $4N_r$ different quantization outputs corresponding to each input symbol. The resulting achievable rate will approach to $\log_2(4N_r)$ as transmission power increases.

C. MIMO Channel with One-Bit Quantization

Proposition 2. For the MIMO channel with one-bit quantization, the high SNR capacity, denoted as $\bar{C}_{\text{MIMO}}(\mathbf{H})$, satisfies,

$$2\text{rank}(\mathbf{H}) \leq \bar{C}_{\text{MIMO}}(\mathbf{H}) \leq 2N_r. \quad (11)$$

Proof: First, since there are at most 2^{2N_r} possible quantization outputs at the receiver, $\bar{C}_{\text{MIMO}}(\mathbf{H}) \leq 2N_r$.

Now we denote the rank of the channel matrix as $n = \text{rank}(\mathbf{H})$. Without loss of generality, assume that the first n rows are linearly independent and define \mathbf{A} as a $n \times N_t$ matrix consisting of these n rows. Consider the quantization outputs of the first $2n$ quantizer, i.e., $\mathbf{r}_{1:2n} := \{r_i, 1 \leq i \leq 2n\}$. For each of the 2^{2n} possible values of $\mathbf{r}_{1:2n}$, there is a corresponding

input symbol $\mathbf{x} = \mathbf{A}^*(\mathbf{A}\mathbf{A}^*)^{-1}\mathbf{y}$ such that $\mathbf{Q}(\mathbf{y}) = \mathbf{r}_{1:2n}$ assuming there is no noise. By transmitting these 2^{2n} signals with equal probability, a lower bound of the channel capacity in the high SNR regime, which is $2n$, is achieved. Thus the proposition is proved. ■

Corollary 2. If the channel coefficients are independently generated from a continuous distribution, then

$$2 \min\{N_r, N_t\} \leq \bar{C}_{\text{MIMO}}(\mathbf{H}) \leq 2N_r. \quad (12)$$

Proof: When the channel coefficients are independently generated from a continuous distribution, then with probability one, $\text{rank}(\mathbf{H}) = \min\{N_r, N_t\}$. Inserting this into (11), we obtain Corollary 2. ■

IV. MMWAVE CHANNEL WITH ONE-BIT QUANTIZATION

Scattering tends to be lower in the mmWave band compared with lower frequencies and thus $\text{rank}(\mathbf{H})$ may be less than $\min\{N_r, N_t\}$. In this section we assume a ray-based channel model with L paths [18], [19]. Denote α_ℓ , $\phi_{r\ell}$, $\phi_{t\ell}$ as the strength, the angle of arrival and the angle of departure of the ℓ th path, respectively. We also assume that uniform linear arrays are deployed at the transmitter and receiver. The array response vector at the receiver can be written as

$$\mathbf{a}_r(\phi_{r\ell}) = \frac{1}{\sqrt{N_r}} [1, e^{j\theta}, e^{j2\theta}, \dots, e^{j(N_r-1)\theta}]^T \quad (13)$$

where $\theta = \frac{2\pi}{\lambda} d \sin(\varphi_{r\ell})$. Herein, λ is the wavelength and d is the inter-element spacing. The array response vector at the transmitter $\mathbf{a}_t(\varphi_{t\ell})$ is defined similarly. Hence, the channel matrix is,

$$\mathbf{H} = \sum_{\ell=1}^L \alpha_\ell \mathbf{a}_r(\varphi_{r\ell}) \mathbf{a}_t^*(\varphi_{t\ell}). \quad (14)$$

Corollary 3. For a MIMO system with channel model in (14), $2 \min\{L, N_r, N_t\} \leq \bar{C}_{\text{MIMO}}(\mathbf{H}) \leq 2N_r$.

Proof: For the channel model shown in (14), $\text{rank}(\mathbf{H}) = \min\{L, N_r, N_t\}$ [20]. Combining this with Proposition 2, we obtain Corollary 3. ■

In mmWave systems, the number of multipaths is limited due to the sparse scattering structure. Meanwhile, large antenna arrays are usually deployed to obtain beamforming gain for combatting the path loss. Hence, in the case when $L < \min\{N_t, N_r\}$, we have $2L \leq \bar{C}_{\text{MIMO}}(\mathbf{H}) \leq 2N_r$. Therefore, multipath is helpful in improving the lower bound of high SNR capacity in a scattering-limited environment.

Next, we consider such a mmWave MIMO channel with only one path and propose a transmission strategy. If $L = 1$, the channel (14) degenerates to

$$\mathbf{H} = \alpha \mathbf{a}_r(\varphi_r) \mathbf{a}_t^*(\varphi_t). \quad (15)$$

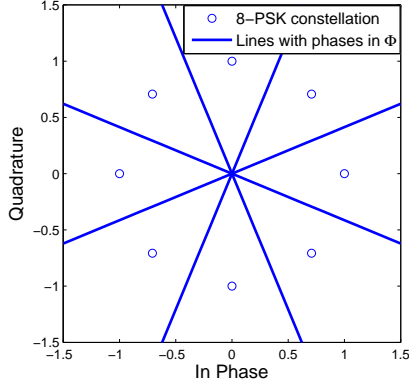


Fig. 3. In our proposed strategy, the transmitter sends 8-PSK symbols and $\Phi = \{\frac{\pi}{8} + k\frac{\pi}{4}, k = 0, 1, \dots, 7\}$ when $N_r = 2$.

To obtain beamforming gain, matched filter beamforming is used at the transmitter and the resulting channel is equivalent to a SIMO channel. The transmitter sends $4N_r$ -PSK symbols since the receiver can at most distinguish $4N_r$ received signals in the high SNR regime. Now we propose a receiver structure for this system. In each antenna, a phase shifter is installed before the quantizers to rotate the received signal. The output of the quantizer is

$$\mathbf{r} = \mathbf{Q}(\mathbf{b}_r \odot (\alpha \mathbf{a}_r(\varphi_r) x + \mathbf{n})), \quad (16)$$

where $\mathbf{b}_r = [e^{j\psi_0}, e^{j\psi_1}, \dots, e^{j\psi_{N_r-1}}]^T$ represents the rotation operation implemented by phase shifters.

In the proof of Proposition 1, we see that the SIMO receiver acts as a phase detector defined by Φ . The whole range $[0, 2\pi]$ is divided into $4N_r$ regions $\{[\phi_m, \phi_{m+1}]\}$ ($0 \leq m \leq 4N_r - 2$) and $[\phi_{4N_r-1}, \phi_0]$ assuming $0 \leq \phi_0 < \phi_1 < \dots < \phi_{4N_r-1} < 2\pi$. A simple and heuristic design is to let the phases of transmitted $4N_r$ -PSK symbols, which are $\{\frac{k\pi}{2N_r}, 0 \leq k \leq 4N_r - 1\}$, fall into each of the $4N_r$ regions. Therefore, we want $\Phi = \{\frac{\pi}{4N_r} + k\frac{\pi}{2N_r}, 0 \leq k \leq 4N_r - 1\}$. This can be achieved by designing \mathbf{b}_r such that

$$\mathbf{b}_r \odot \mathbf{a}_r(\varphi_r) = \frac{1}{\sqrt{N_r}} e^{j\frac{\pi}{4N_r}} [1, e^{j\frac{\pi}{2N_r}}, e^{j\frac{2\pi}{2N_r}}, \dots, e^{j\frac{(N_r-1)\pi}{2N_r}}]^T.$$

We plot the case when $N_r = 2$ in Fig. 3. The transmitter sends 8-PSK symbols. By appropriately designing \mathbf{b}_r , the resulting Φ is $\{\frac{\pi}{8} + k\frac{\pi}{4}, k = 0, 1, \dots, 7\}$. In Fig. 3, each of the 8-PSK symbols is on the angular bisector of the lines with phases in Φ .

V. SIMULATION RESULTS

A. SIMO Channel with One-Bit Quantization

In the SIMO channel, we obtain the capacity-achieving input distribution using the cutting plane method [21, Sec. IV-A]. For this method, we take a fine quantized discrete grid on the region $\{x : -3\sqrt{P} \leq \Re\{x\} \leq 3\sqrt{P}, -3\sqrt{P} \leq \Im\{x\} \leq 3\sqrt{P}\}$ as the possible inputs and optimize their probabilities. In Fig. 4, we shown a simple case when $\mathbf{h} = [e^{j\pi/8}, e^{-j\pi/8}]^T$. It is interesting to find that the optimal input constellation

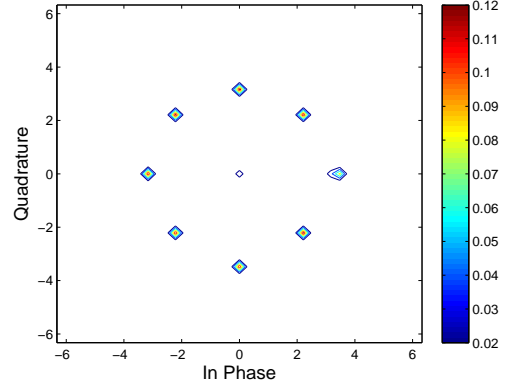


Fig. 4. The optimal input distribution of the SIMO channel when $\mathbf{h} = [e^{j\pi/8}, e^{-j\pi/8}]^T$. The transmission power $P = 10$ and the achieved rate is about 2.52 bps/Hz.

contains the rotated 8-PSK symbols and the symbol zero. For other channels, the optimal constellation may not be regular.

B. MIMO Channel with One-Bit Quantization

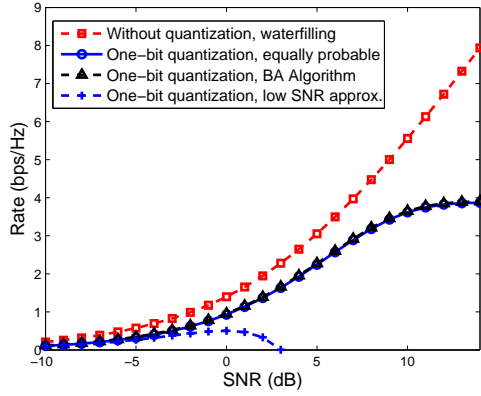
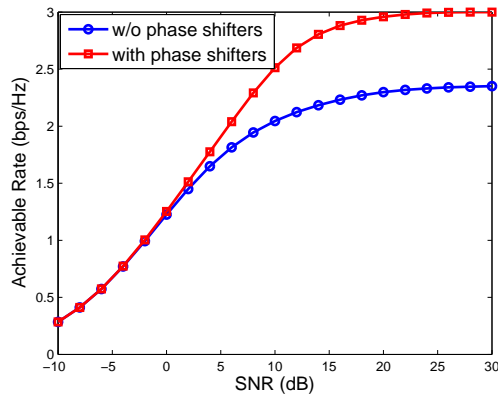
In Fig. 5, we plot the achievable rate when $N_t = N_r = 2$. The channel coefficients are generated from $\mathcal{CN}(0, 1)$ distribution independently and the results are obtained by averaging over 100 different channel realizations. The input alphabet, which contains $2^{2N_r} = 16$ input symbols, are constructed by the method used in the proof of Proposition 2. The input symbols are obtained by solving

$$\mathbf{x} = \sqrt{P} \frac{\mathbf{H}^{-1} \mathbf{y}}{\|\mathbf{H}^{-1} \mathbf{y}\|}, \quad (17)$$

where $\mathbf{y} = [\pm 1 \pm j, \pm 1 \pm j]^T$. These symbols are transmitted with equal probabilities $1/16$ or with probabilities optimized by the Blahut-Arimoto algorithm [22]. We can see that these two curves are very close in Fig. 5. The channel capacity without quantization is computed using the usual waterfilling approach. When the SNR is less than 5dB, the gap between the curves with and without quantization is small. When the SNR is larger than 5dB, the achievable rate with one-bit quantization approaches the upper bound 4 bps/Hz. In Fig. 5, we also plot the low SNR capacity approximation given by [15, Eq. (18)]. We see that when SNR is less than -5 dB, the curve of low SNR approximation is close to the other two curves of one-bit quantization. In the high SNR regime, however, it will be negative and far away from the other curves.

C. MmWave Channel with One-Bit Quantization

In this part, we evaluate the performance of our proposed transmission strategy in a 2×2 channel with single path. We assume that the angles of departure φ_t and angles of arrival φ_r are uniformly distributed. The complex path gains α is Gaussian distributed. The inter-element spacing of the receiver antenna array is set to one quarter of the wavelength. The transmitter employs 8-PSK signaling. If there is no phase shifter, the received complex signals are directly quantized by the one-bit ADCs. If the receiver has one phase shifter on each

Fig. 5. Achievable rate of the 2×2 MIMO channel.Fig. 6. The achievable rate with the proposed transmission strategy in a mmWave 2×2 channel with only one path.

receiver antenna, the phase shifters will rotate the phase of the input signals such that $\Phi = \{\frac{\pi}{8} + k\frac{\pi}{4}, k = 0, 1, \dots, 7\}$. In Fig. 6, we compare the performances of the above two receiver structures. The proposed receiver structure can achieve higher rate in medium and high SNR regimes. Note that the phase shifters are potentially as power efficient as one-bit ADCs [23]. Therefore, our proposed receiver structure achieves higher performance with little increase of power consumption. The gains may be smaller for larger numbers of receive antennas.

VI. CONCLUSION

In this paper, we studied the capacity of point-to-point MIMO channel with one-bit quantization at the receiver. We found that the high SNR capacity of SIMO channel increase linearly with $\log_2(N_r)$. For the MIMO channel, the high SNR capacity is lower bounded by the rank of the channel. We also considered the mmWave MIMO channel with limited scattering. We showed that multipath is helpful in improving the lower bound of the high SNR capacity. Finally, we proposed a power efficient receiver structure where the phase shifters and one-bit ADCs are used to achieve higher data rate.

ACKNOWLEDGEMENT

This material is based upon work supported in part by the National Science Foundation under Grant Nos. NSF-CCF-

REFERENCES

- [1] R. Walden, "Analog-to-digital converter survey and analysis," *IEEE J. Sel. Areas Commun.*, vol. 17, no. 4, pp. 539–550, 1999.
- [2] B. Murmann, "ADC performance survey 1997-2013." [Online]. Available: <http://www.stanford.edu/~murmann/adcsurvey.html>
- [3] S. Vitali, G. Cimatti, R. Rovatti, and G. Setti, "Adaptive time-interleaved ADC offset compensation by nonwhite data chopping," *IEEE Trans. Circuits Syst. II*, vol. 56, no. 11, pp. 820–824, 2009.
- [4] S. Ponnuru, M. Seo, U. Madhow, and M. Rodwell, "Joint mismatch and channel compensation for high-speed OFDM receivers with time-interleaved ADCs," *IEEE Trans. Commun.*, vol. 58, no. 8, pp. 2391–2401, 2010.
- [5] T. Sundstrom, B. Murmann, and C. Svensson, "Power dissipation bounds for high-speed nyquist analog-to-digital converters," *IEEE Trans. Circuits Syst. I*, vol. 56, no. 3, pp. 509–518, 2009.
- [6] J. Singh, S. Ponnuru, and U. Madhow, "Multi-gigabit communication: the ADC bottleneck," in *IEEE International Conference on Ultra-Wideband*, 2009, pp. 22–27.
- [7] O. Dabeer, J. Singh, and U. Madhow, "On the limits of communication performance with one-bit analog-to-digital conversion," in *IEEE 7th Workshop on Signal Processing Advances in Wireless Communications*, 2006, pp. 1–5.
- [8] J. Singh, O. Dabeer, and U. Madhow, "On the limits of communication with low-precision analog-to-digital conversion at the receiver," *IEEE Trans. Commun.*, vol. 57, no. 12, pp. 3629–3639, 2009.
- [9] S. Krone and G. Fettweis, "Capacity of communications channels with 1-bit quantization and oversampling at the receiver," in *2012 35th IEEE Sarnoff Symposium (SARNOFF)*, 2012, pp. 1–7.
- [10] G. Zeitler, A. Singer, and G. Kramer, "Low-precision A/D conversion for maximum information rate in channels with memory," *IEEE Trans. Commun.*, vol. 60, no. 9, pp. 2511–2521, 2012.
- [11] O. Dabeer and U. Madhow, "Channel estimation with low-precision analog-to-digital conversion," in *2010 IEEE International Conference on Communications (ICC)*, 2010, pp. 1–6.
- [12] G. Zeitler, G. Kramer, and A. Singer, "Bayesian parameter estimation using single-bit dithered quantization," *IEEE Trans. Signal Process.*, vol. 60, no. 6, pp. 2713–2726, 2012.
- [13] A. Wadhwa and U. Madhow, "Blind phase/frequency synchronization with low-precision ADC: a Bayesian approach," in *Proc. of 51st Allerton Conference on Communication Control and Computing*, 2013.
- [14] M. Ivrlac and J. Nosssek, "Challenges in coding for quantized MIMO systems," in *2006 IEEE International Symposium on Information Theory*, July 2006, pp. 2114–2118.
- [15] A. Mezghani and J. Nosssek, "On ultra-wideband MIMO systems with 1-bit quantized outputs: Performance analysis and input optimization," in *IEEE International Symposium on Information Theory*, 2007, pp. 1286–1289.
- [16] —, "Analysis of Rayleigh-fading channels with 1-bit quantized output," in *IEEE International Symposium on Information Theory*, 2008, pp. 260–264.
- [17] —, "Analysis of 1-bit output noncoherent fading channels in the low SNR regime," in *IEEE International Symposium on Information Theory*, 2009, pp. 1080–1084.
- [18] O. El Ayach, S. Rajagopal, S. Abu-Surra, Z. Pi, and R. Heath, "Spatially sparse precoding in millimeter wave mimo systems," *IEEE Trans. Wireless Commun.*, vol. PP, no. 99, pp. 1–15, 2014.
- [19] A. Alkhatib, O. El Ayach, G. Leus, and R. W. Heath Jr, "Hybrid precoding for millimeter wave cellular systems with partial channel knowledge," in *Proc. of Information Theory and Applications (ITA) Workshop*, 2013.
- [20] G. Raleigh and J. Cioffi, "Spatio-temporal coding for wireless communication," *IEEE Trans. Commun.*, vol. 46, no. 3, pp. 357–366, Mar 1998.
- [21] J. Huang and S. Meyn, "Characterization and computation of optimal distributions for channel coding," *IEEE Trans. Inf. Theory*, vol. 51, no. 7, pp. 2336–2351, 2005.
- [22] R. Blahut, "Computation of channel capacity and rate-distortion functions," *IEEE Trans. Inf. Theory*, vol. 18, no. 4, pp. 460–473, 1972.
- [23] C. Doan, S. Emami, D. Sobel, A. Niknejad, and R. Brodersen, "Design considerations for 60 GHz CMOS radios," *IEEE Commun. Mag.*, vol. 42, no. 12, pp. 132–140, Dec 2004.